Electronic supplementary information

The role of SP-$B_{1\text{-}25}$ peptides in lung surfactant monolayers exposed to gold nanoparticles

SHEIKH I. HOSSAIN[1], NEHA S. GANDHI[2], ZAK E. HUGHES[3], SUVASH C. SAHA[1*]

[1]School of Mechanical and Mechatronic Engineering, University of Technology Sydney, 81 Broadway, Ultimo NSW 2007, Australia
[2]School of Mathematical Sciences, Queensland University of Technology, 2 George Street, GPO Box 2434, Brisbane QLD 4001,
[3]School of Chemistry and Biosciences, The University of Bradford, Bradford, BD7 1DP, UK
*corresponding author: suvash.saha@uts.edu.au

Section S1: Methodological Details of Analyses:

Mean-squared displacement and lateral diffusion coefficient

The lung surfactant (LS) phospholipids' (PLs) lateral diffusion coefficient were calculated from the slope of the mean square displacement (MSD) over time. The following equation expresses the MSD

$$MSD\ (t) = \Delta r_i(t) = < \left[r_i(t + t_0) - r_i(t_0) \right]^2 > \quad (1s)$$

where at time t, the i^{th} particle position is $r(t)$, and $r(t_o)$ the position of the particle at time t_0. The angle brackets designate a time-average over t and overall molecules. Therefore, the diffusion coefficient D is defined by

$$D = \lim_{t \to \infty} \frac{1}{2dt} MSD(t) \quad (2s)$$

where d is the dimensionality of diffusion (here $d = 2$), which means we calculate the lateral diffusion coefficients and MSD in a plane perpendicular to Z-axis.

Surface tension

We calculated the surface tension for each monolayer of the systems with concentrations (~0.19, ~0.58, ~0.86, and ~1.53 mol %) of polydisperse AuNPs/lipids by using diagonal components of pressure tensor:

$$\gamma = \frac{L_z \left(P_{zz} - \frac{P_{xx} + P_{yy}}{2} \right)}{2} \quad (3s)$$

where

$\gamma =$ Monolayer surface tension

$L_z =$ Box length in the normal direction

$P_{zz} =$ Pressure along the normal of the monolayer

$\frac{P_{xx} + P_{yy}}{2} =$ Lateral pressure

The factor of one half was used in Equation 3s as each system consisting of two monolayers. The block averaging method[1] was used to estimate the error of each single run, with estimated errors in line with those reported by previous coarse-grained simulation studies.[2] The final uncertainties reported were determined from the standard deviation of the parameter over the repeated simulation runs for that system. We used Berendsen pressure barostat[3] with surface tension coupling as Parrinello-Rahman barostat[4] with surface tension coupling is not implemented in GROMACS version 5.1.4 [5].

Order parameter

The PLs (tail beads) order parameter values were computed to investigate the structural orientation/flexibility of PLs in the monolayer under different monolayer conditions. The order parameter of the monolayer PLs tail beads can be defined by the following formula,

$$S_z = \frac{3}{2}\left(< \cos^2 \theta > - \frac{1}{3} \right) \quad (4s)$$

where S_z is the order parameter, θ is the angle between lipid tail beads bonds and monolayer normal [6], angular brackets designates the average of ensemble between temporal and molecular ensembles.[7] The order parameter value ranges $-0.5 \leq S_z \leq 1$. The value $S_z = 1$ indicates that the PL tails are perfect alignment and parallel to the monolayer normal, and a value $S_z = -0.5$ indicates that the PL tails are perfect anti-alignment and perpendicular to the monolayer normal. In our calculation of lipid order parameters, we have used a standard conversion factor of 4 to the python script do-order-gmx5.py from MARTINI website[8], as reported in previous studies.[9-11]

Comparison of POPG and POPC containing LS monolayers

In our model, we used POPG over the other abundant surfactant component POPC (1-palmitoyl-2-oleoyl-sn-glycero-3-phosphocholine) to make consistent our model with previous experimental (*in vitro*) study by Bakshi *et al.*[12]. In addition, we found comparison of simulations of DPPC+POPC LS models with DPPC+POPG models show close agreement. For example, the area per lipid of our control system DPPC+POPG [10] is in good agreement with the data reported in Estrada-López *et al*. [13]. In addition, there is no significant difference in these two phospholipids tails order parameter values (Fig. S1) at surface tension 0 mN/m.

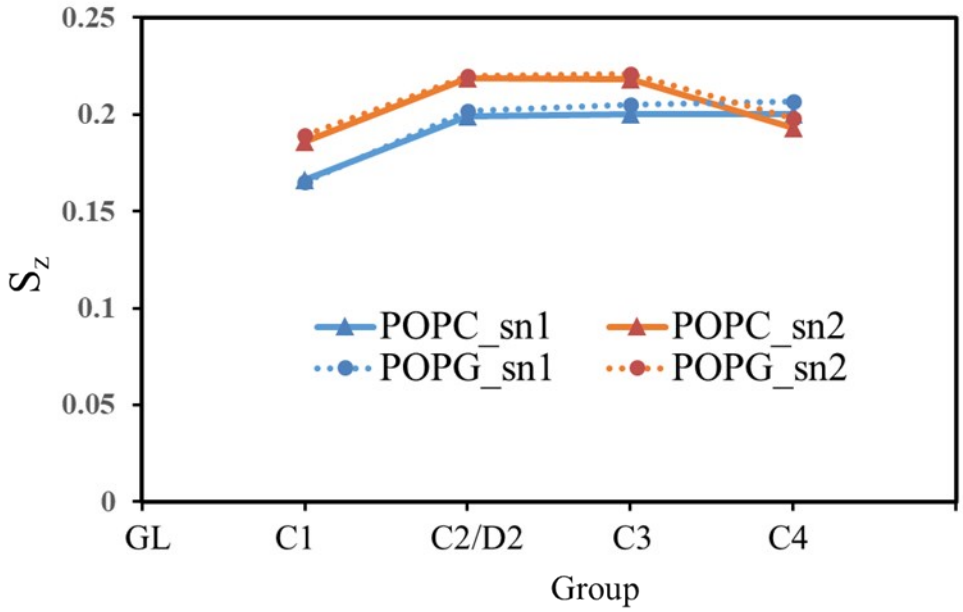

Fig. S1 Order parameter calculation for POPC (solid lines with triangle) and POPG (dash lines with circle) lipids chain 1 (sn1 is in blue colour) (b) chain 2 (sn2 is in orange colour) at surface tension 0 mN/m of the monolayer systems consist of DPPC, POPC and DPPC, POPG.

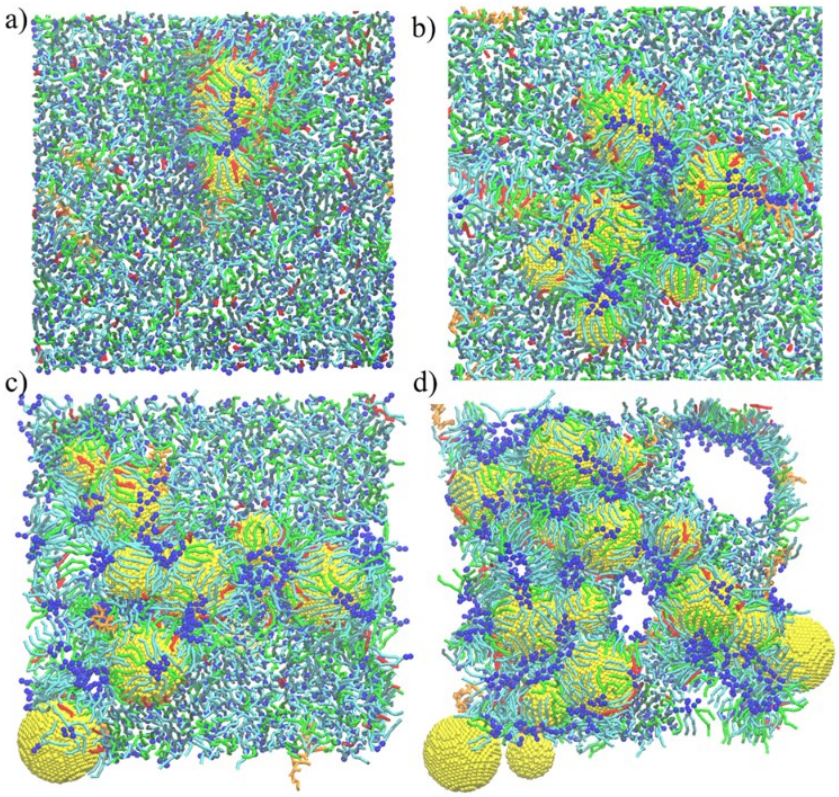

Fig. S2 Pore formation in the surfactant monolayer in state II at different concentrations of AuNPs (a) ~0.19 mol% of AuNPs/lipids, (b) ~0.58 mol% of AuNPs/lipids, (c) ~0.86 mol% of AuNPs/lipids, and (d) ~1.53 mol% of AuNPs/lipids. In all cases, the snapshots are taken after 2 μs simulation.

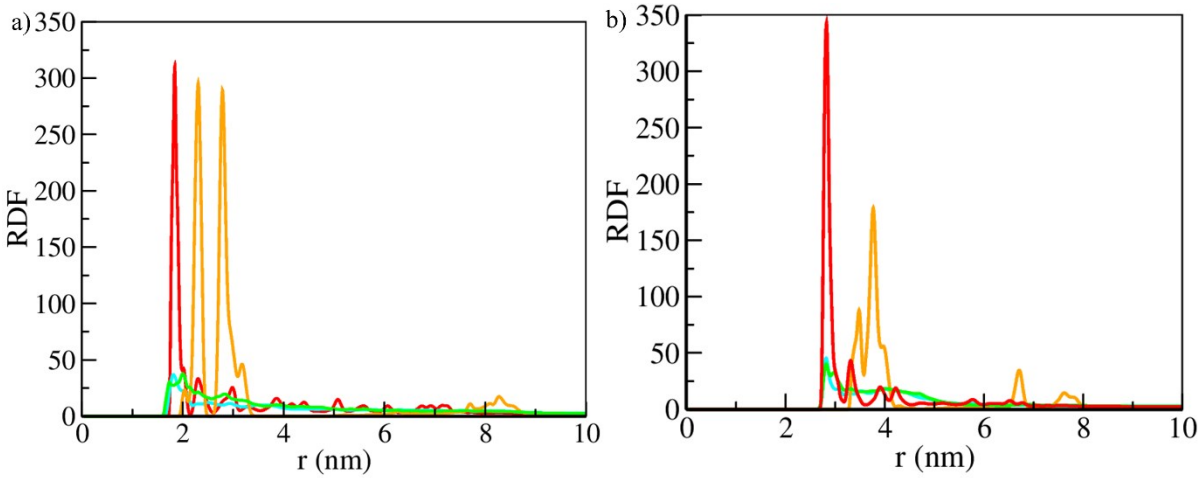

Fig. S3 Radial distribution function (RDF) of surfactant lipids to the two different sizes AuNPs (a) 3 nm and (b) 5 nm in model surfactant monolayer system in presence of polydisperse AuNPs at concentration of (~0.19 mol% of AuNPs/lipids) is shown. The RDF of surfactant lipids (DPPC is in cyan, POPG is in green, CHOL is in red and SP-$B_{1\text{-}25}$ is in orange colours) is calculated over the last 1μs of simulation. The RDF values were calculated from the centre of mass of each surfactant component to the centre of mass of reference AuNP (i.e. mol-mol).

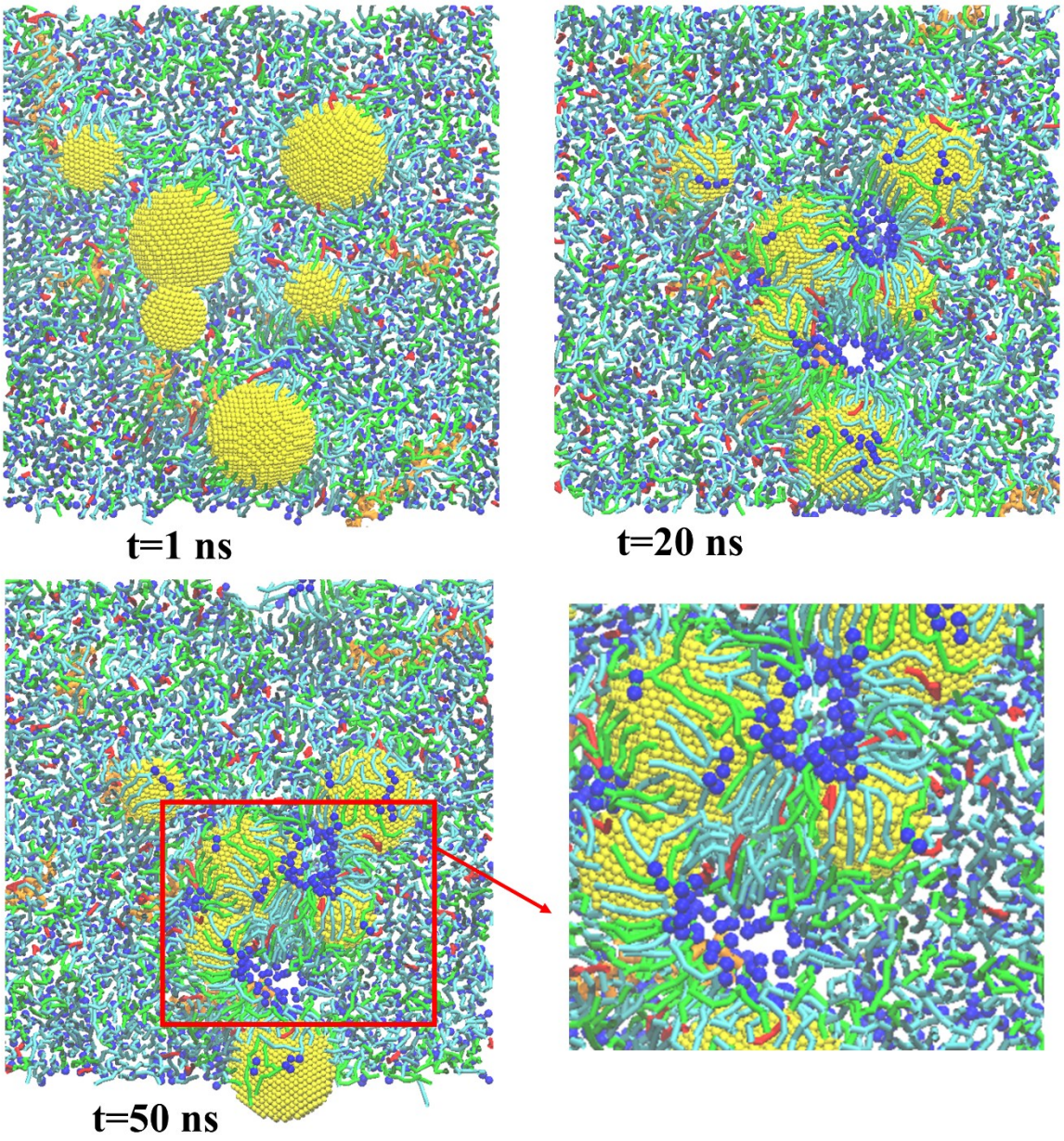

Fig. S4 Representative snapshots showing the aggregation of AuNPs in the LS monolayer in the state I with two different sizes (3 nm and 5 nm) AuNPs at a concentration ~0.58 mol% of AuNPs/lipids. The reverse micelles formation near the aggregated NPs were seen throughout the simulation. The AuNPs are shown as yellow spheres, DPPC as cyan, POPG as green, CHOL as red, SP-$B_{1\text{-}25}$ as orange, and PLs head beads as blue.

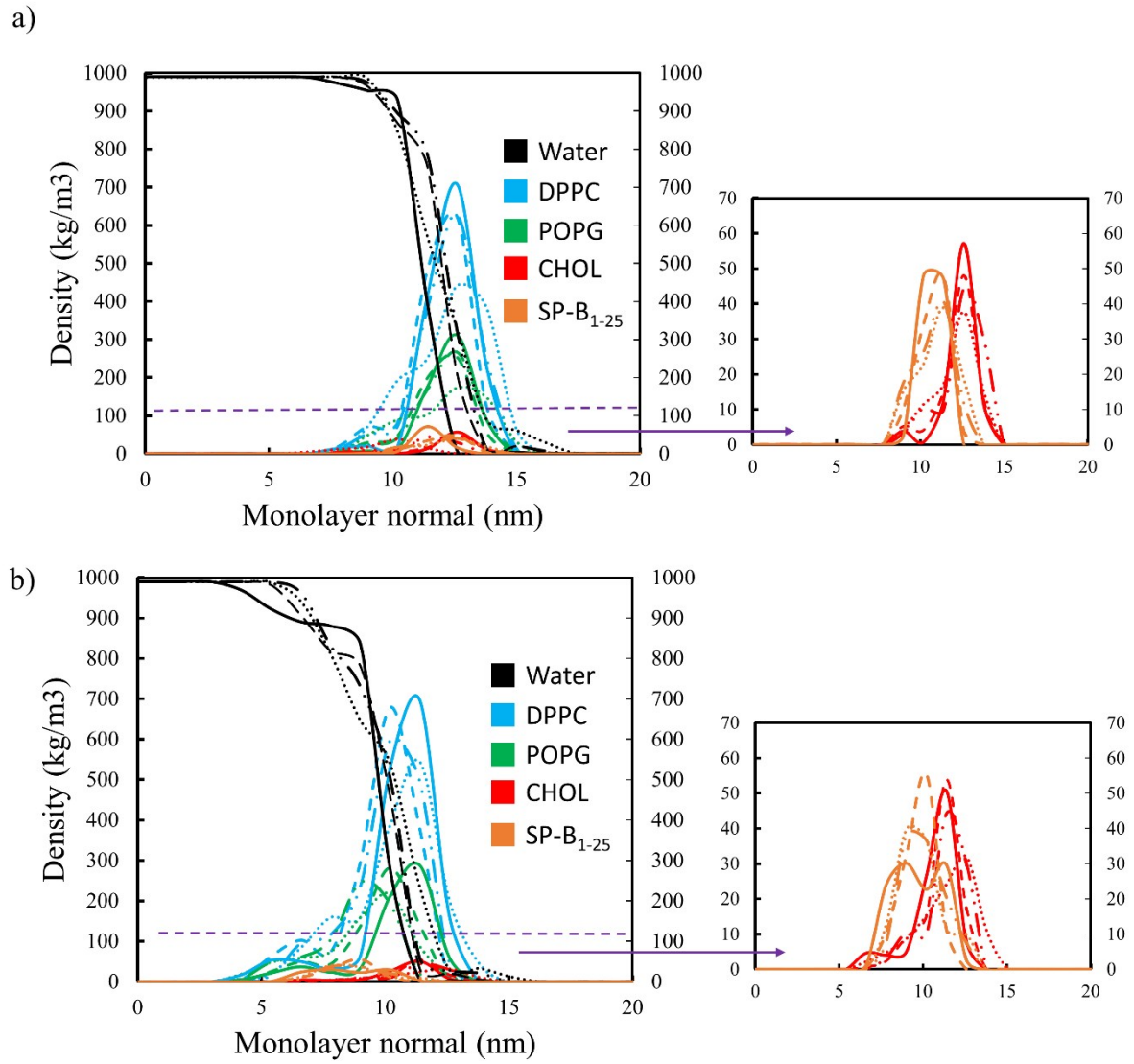

Fig. S5 Density profiles of individual components of model surfactant monolayer (DPPC:POPG:CHOL:SP-B_{1-25}) in (a) state I and (b) state II at different concentrations (~0.19, ~0.58, ~0.86 and ~1.53 mol % of AuNPs/lipids) of polydispersed AuNPs. SP-B_{1-25} and cholesterol densities are presented in insets. Solid line represents ~0.19 mol % of AuNPs/lipids, dash line represents ~0.58 mol % AuNPs/lipids, dash-dotted line represents ~0.86 mol % of AuNPs/lipids, and dotted line represents ~1.53 mol % of AuNPs/lipids concentrations.

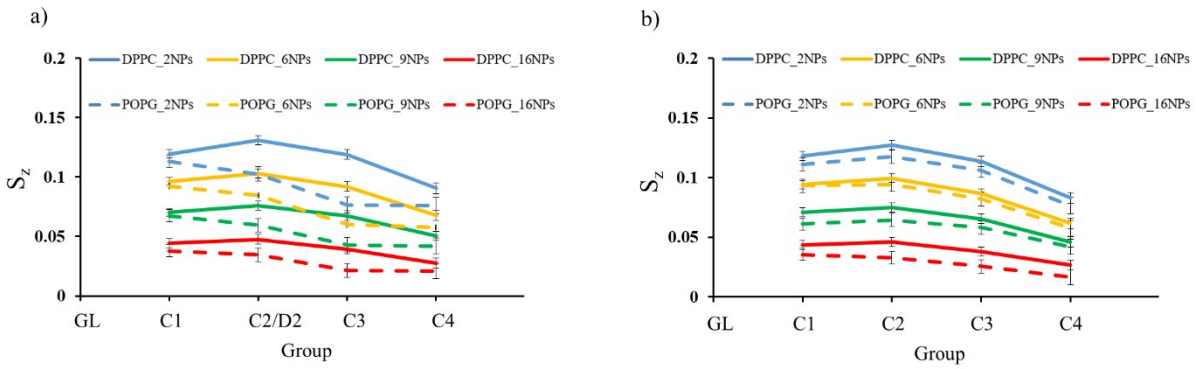

Fig. S6 Order parameter calculation for DPPC (solid lines) and POPG (dash lines) lipids (a) chain 1 (*sn*-1) (b) chain 2 (*sn*-2) at different concentrations of AuNPs (~0.19-~1.53 mol % of AuNPs/lipids) in the monolayer in state III. The error bars have been calculated using the standard deviation across repeated runs.

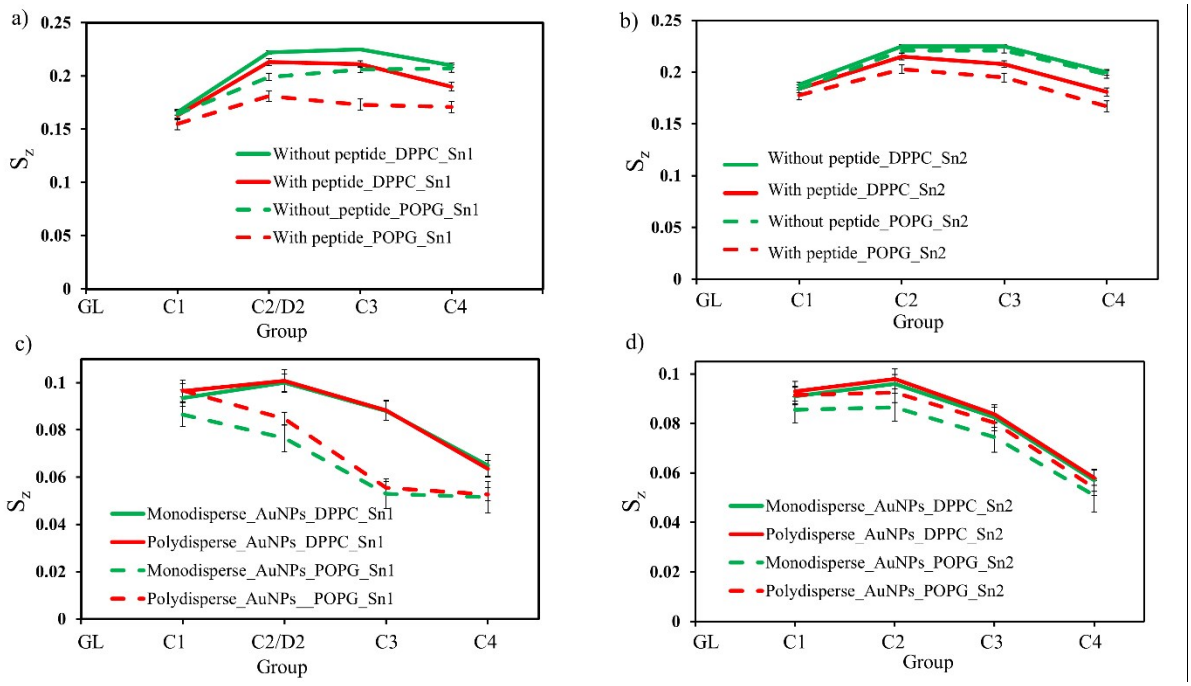

Fig. S7 Order parameter calculation for DPPC (solid lines) and POPG (dash lines) lipids (a,c) chain 1 (*sn*-1) and (b,d) chain 2 (*sn*-2) showing the effects of peptides in the monolayer. Results are only shown for systems at surface tension 0 mN/m; and AuNPs polydispersity at the concentration of AuNPs (~0.58 mol % of AuNPs/lipids) in the monolayer in state II (c,d). Phospholipid order parameters coloured green correspond to the systems in the presence of monodisperse AuNPs and without SP-$B_{1\text{-}25}$. The red colour represents the systems in the presence of polydisperse AuNPs and SP-$B_{1\text{-}25}$. The error bars have been calculated using the standard deviation across repeated runs.

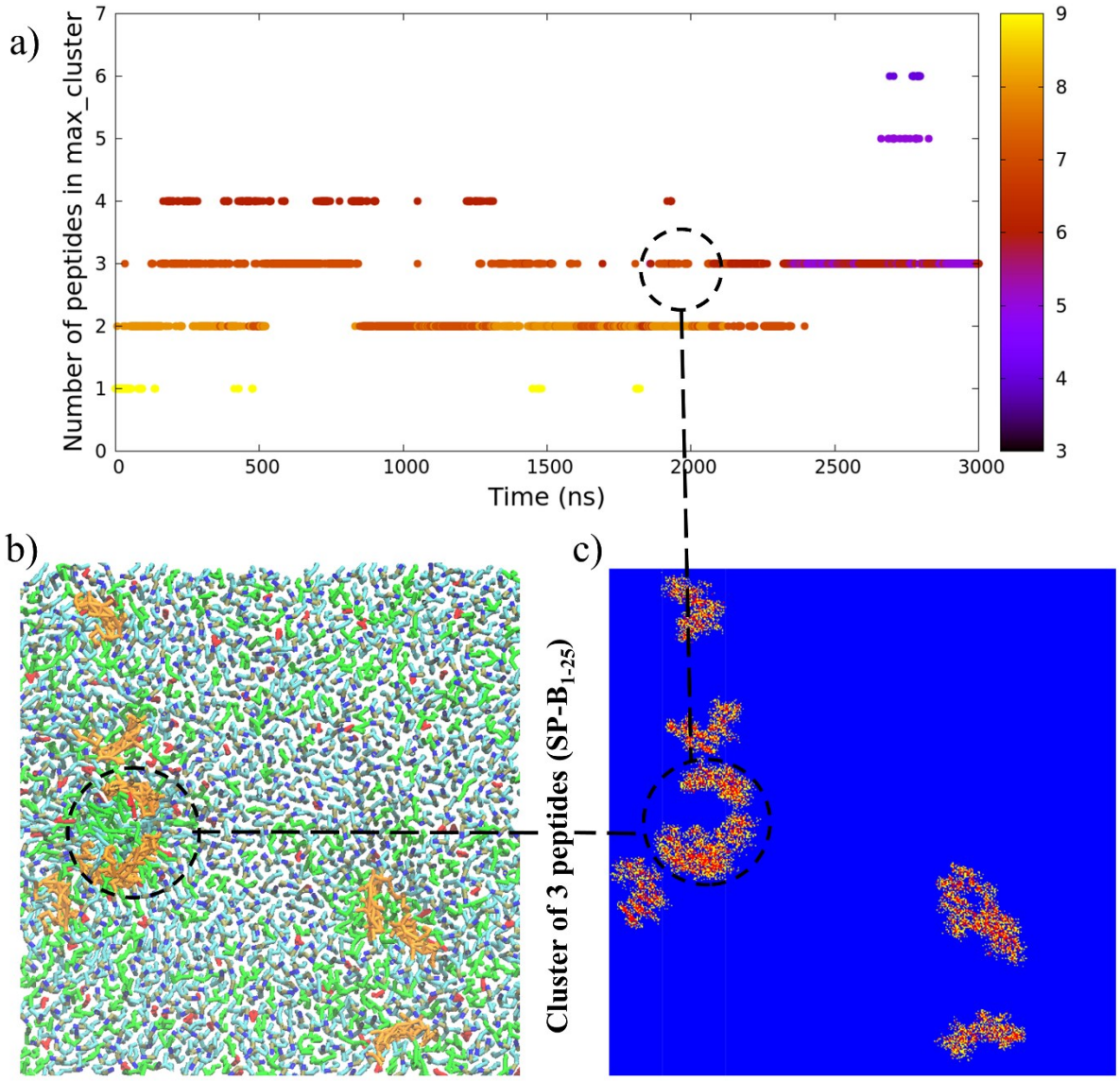

Fig. S8 (a) Cluster size analysis of surfactant peptide B ($SP\text{-}B_{1\text{-}25}$) during surfactant monolayer compression (surface tension 0 mN/m) in the absence of NPs, simulation time is presented along X-axis, the number of $SP\text{-}B_{1\text{-}25}$ in the largest cluster is presented along Y-axis and the number of clusters is presented along Z-axis, (b) top view showing $SP\text{-}B_{1\text{-}25}$ clustering in the surfactant monolayer, and (c) $SP\text{-}B_{1\text{-}25}$ number density map after 2 µs of simulation.

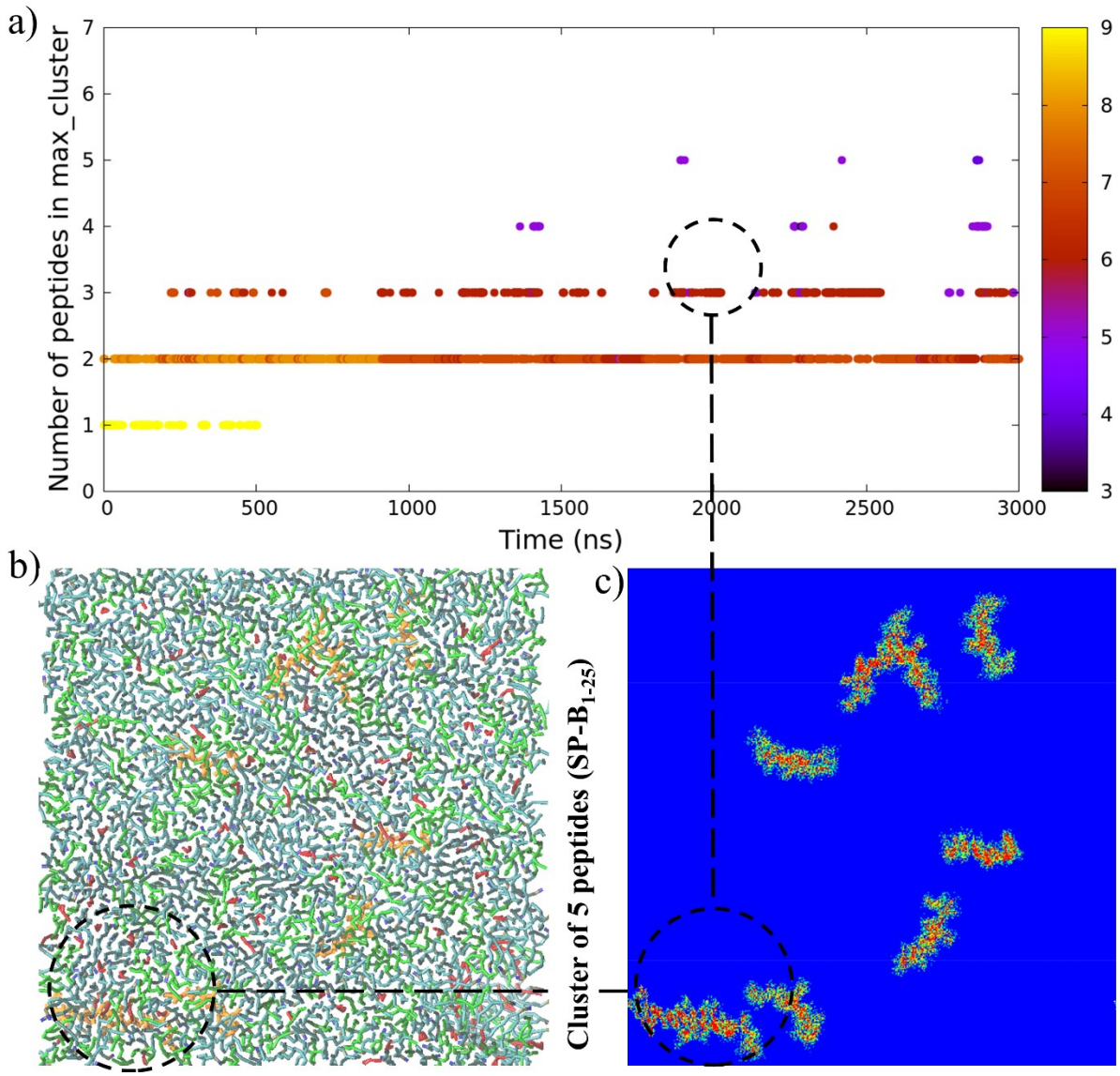

Fig. S9 Cluster size analysis of surfactant peptide B (SP-$B_{1\text{-}25}$) during surfactant monolayer is in state I of the system with AuNPs concentration of ~0.19 mol% of AuNPs/lipids, (a) simulation time is presented along X-axis, the number of SP-$B_{1\text{-}25}$ in the largest cluster is presented along Y-axis, and the number of clusters is presented along Z-axis, (b) visualization of SP-$B_{1\text{-}25}$ clustering in the surfactant monolayer (top view), and (c) SP-$B_{1\text{-}25}$ number density map after 2 μs of simulation.

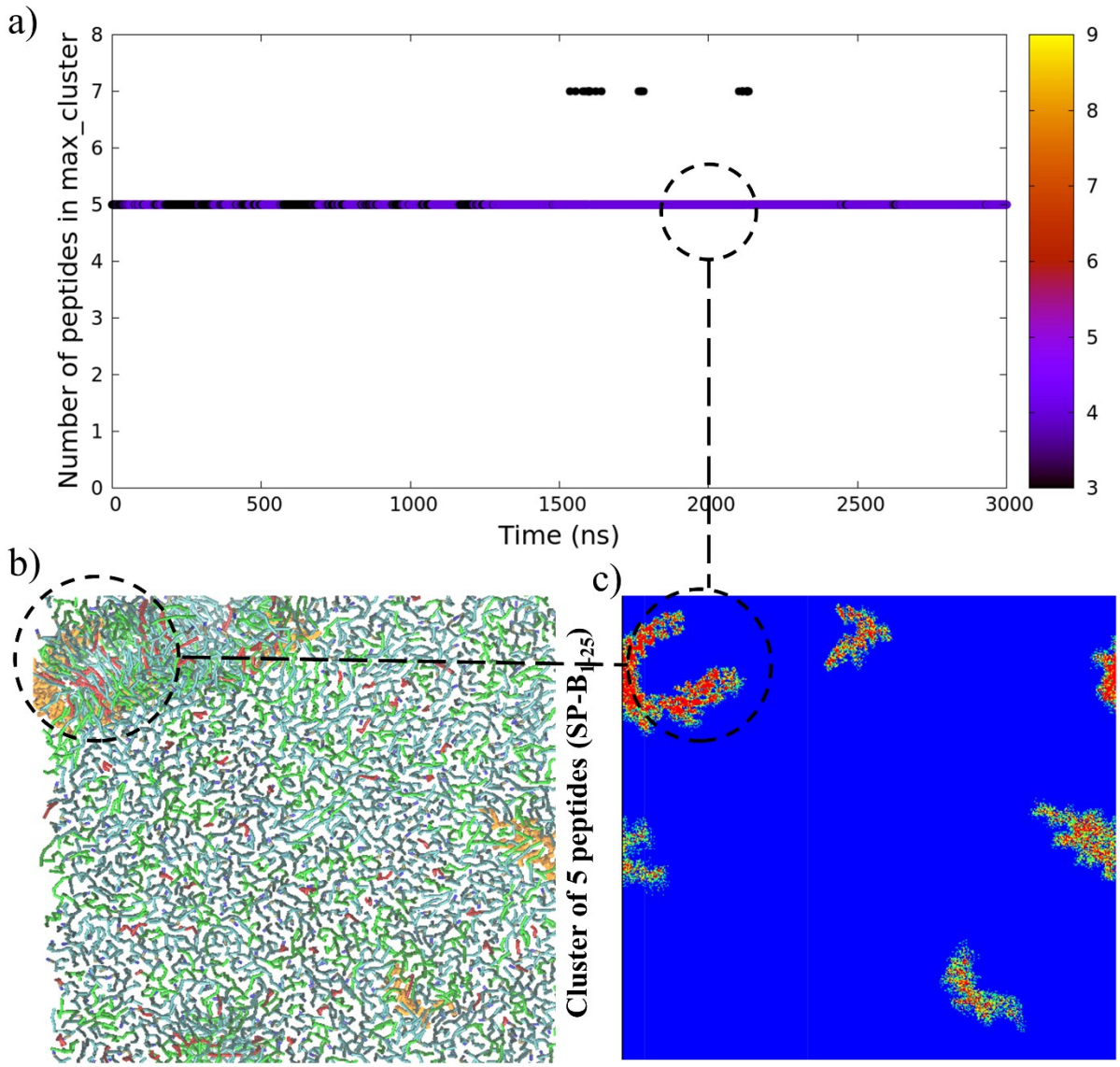

Fig. S10 Cluster size analysis of surfactant peptide B (SP-B_{1-25}) during surfactant monolayer is in state III of the system with AuNPs concentration of ~0.19 mol% of AuNPs/lipids, (a) simulation time is presented along X-axis, the number of SP-B_{1-25} in the largest cluster is presented along Y-axis and the number of clusters is presented along Z-axis, (b) visualization of SP-B_{1-25} clustering in the surfactant monolayer (top view), and (c) SP-B_{1-25} number density map after 2 μs of simulation.

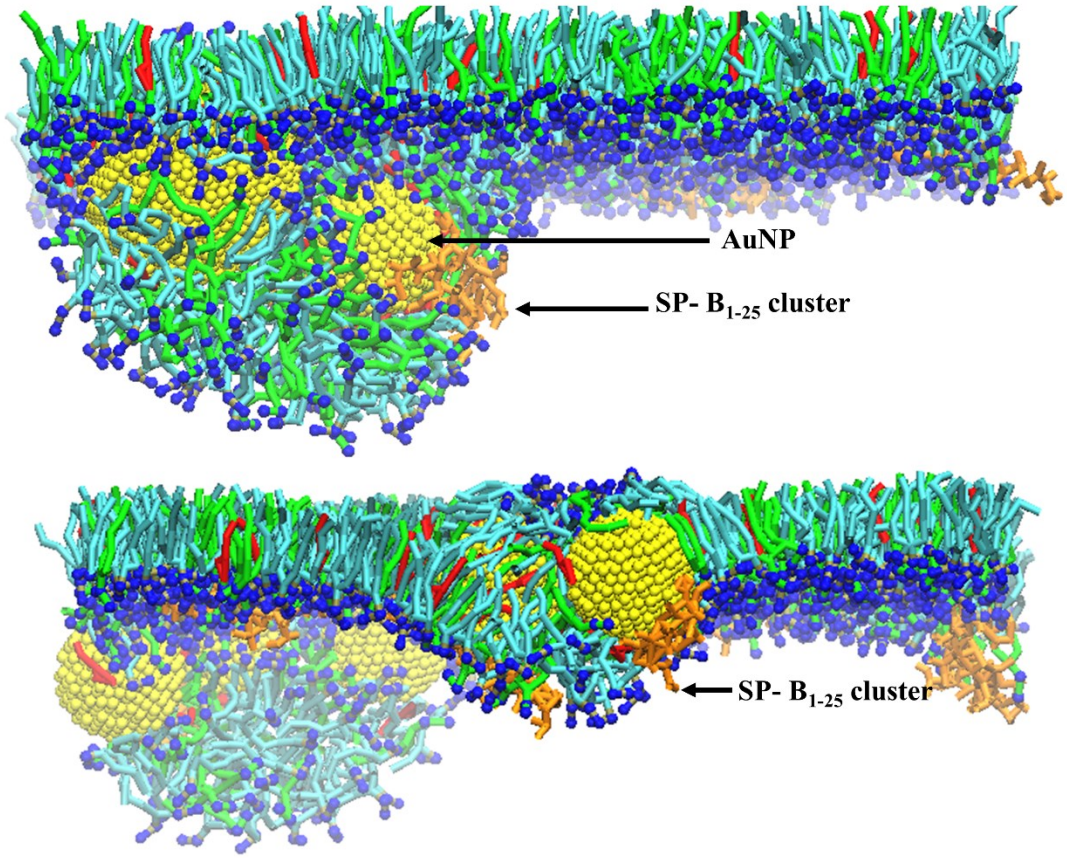

Fig. S11 Interaction between SP-B_{1-25} (shown in orange) and the AuNPs (shown as spheres in yellow) showing the formation of peptide clusters around the AuNPs and lipid head beads, which indicate lipoprotein corona formation in the monolayer. Data is shown for state II monolayers with an AuNP concentration of ~0.58 mol% of AuNPs/lipids: (a) polydisperse AuNPs (b) monodisperse AuNPs. The DPPC is shown as cyan, POPG as green, CHOL as red, and PLs head beads as blue.

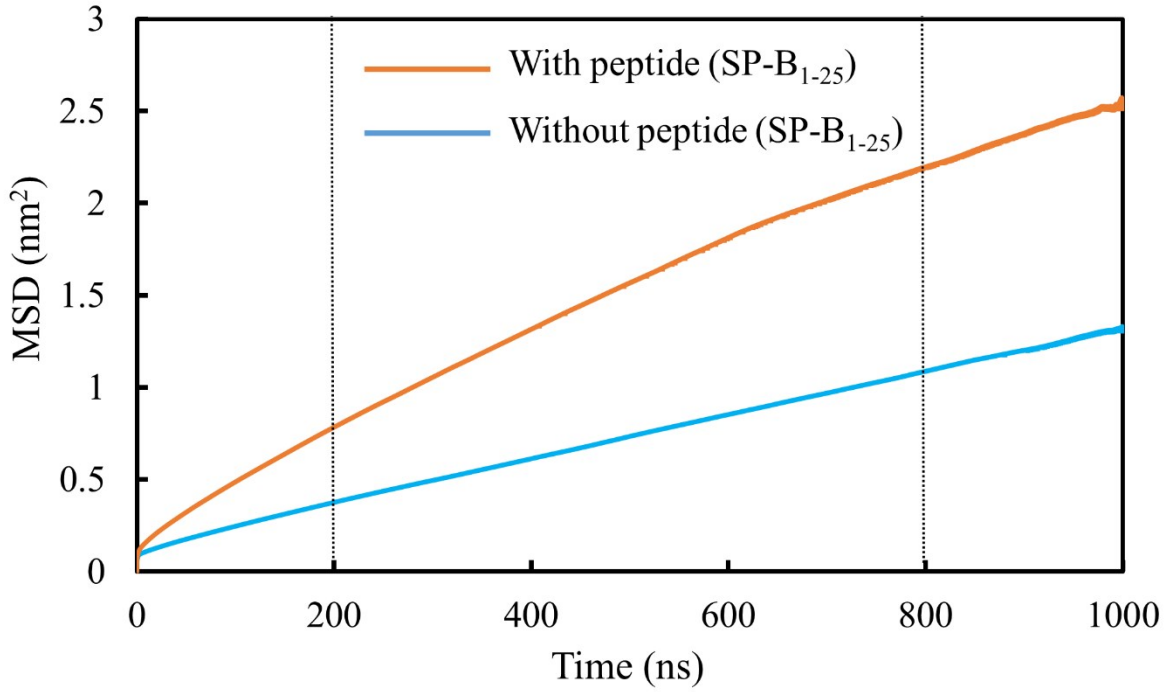

Fig. S12 Effect of surfactant peptide SP-$B_{1\text{-}25}$ on PLs MSD in the monolayer (without NPs) at surface tension 0 mN/m, with (orange) and without SP-$B_{1\text{-}25}$ (blue). The MSD curves were fitted within the time range denoted by the dotted lines.

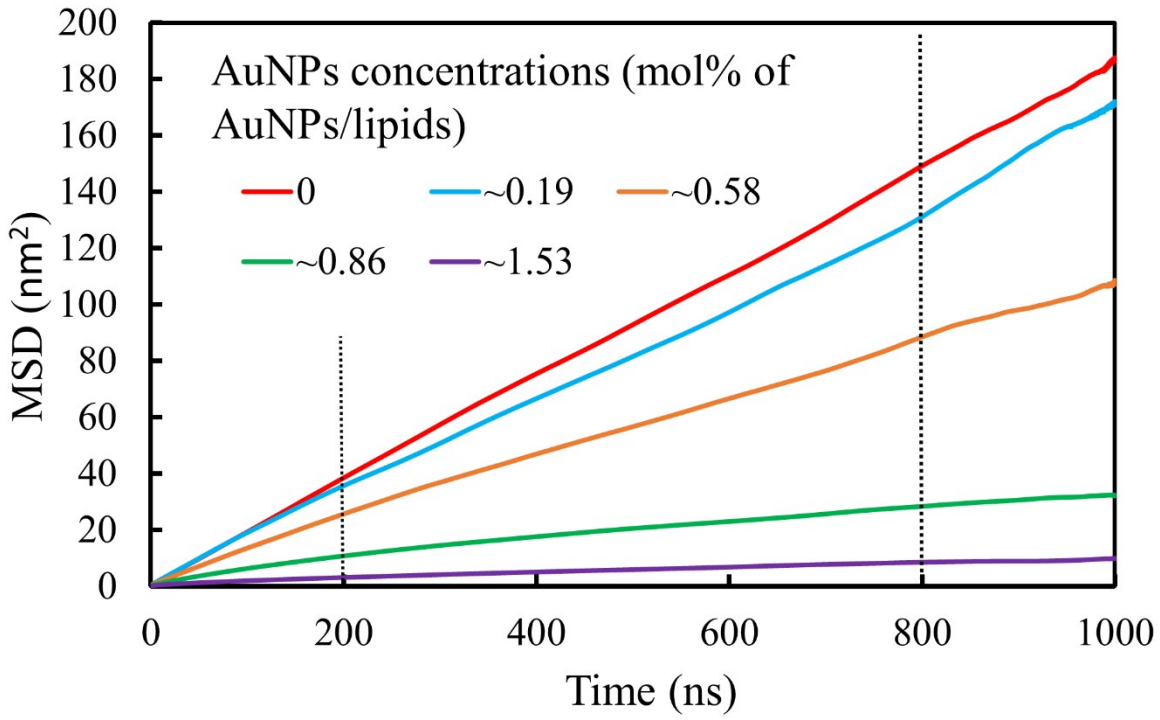

Fig. S13 Lung surfactant monolayer PLs MSD curves, with colours representing to different AuNPs concentrations **0**, ~0.19, ~0.58, ~0.86, and ~1.53 mol% of AuNPs/lipids applied in the monolayer in state I. The time range used for fitting the MSD curves with two dotted lines.

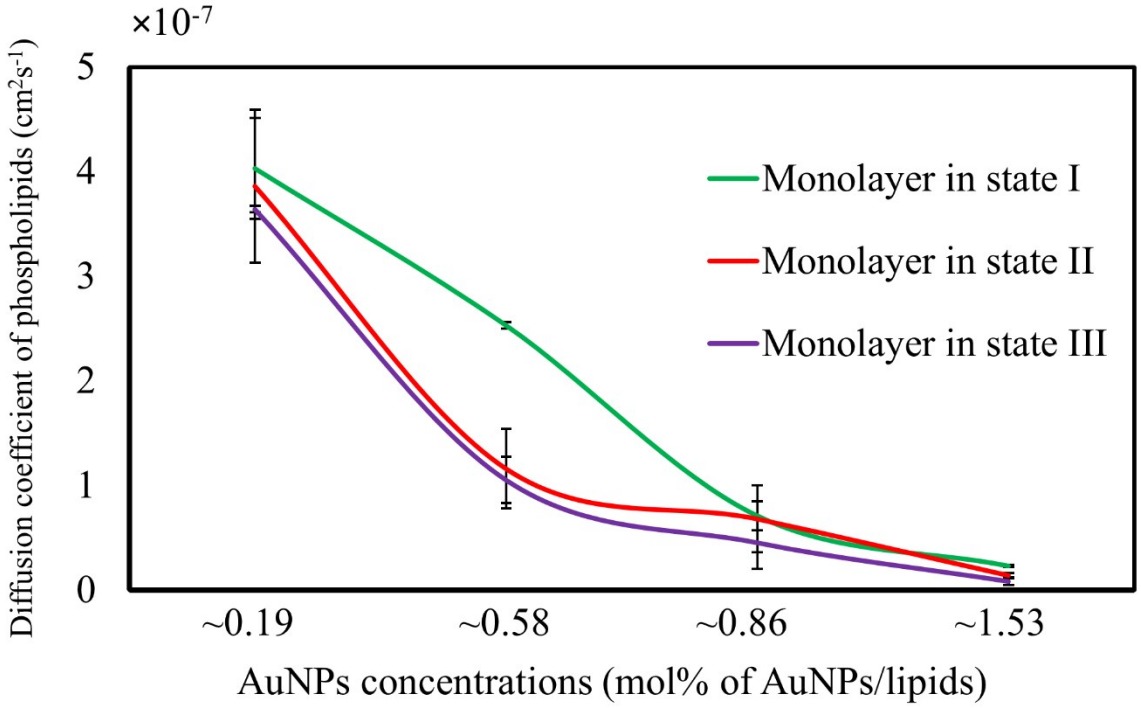

Fig. S14 2D diffusion coefficients of PLs at different AuNPs concentrations, with different colours corresponding different monolayers states; I (green), II (red), and III (purple). The error bars have been calculated using the standard deviation across repeated runs.

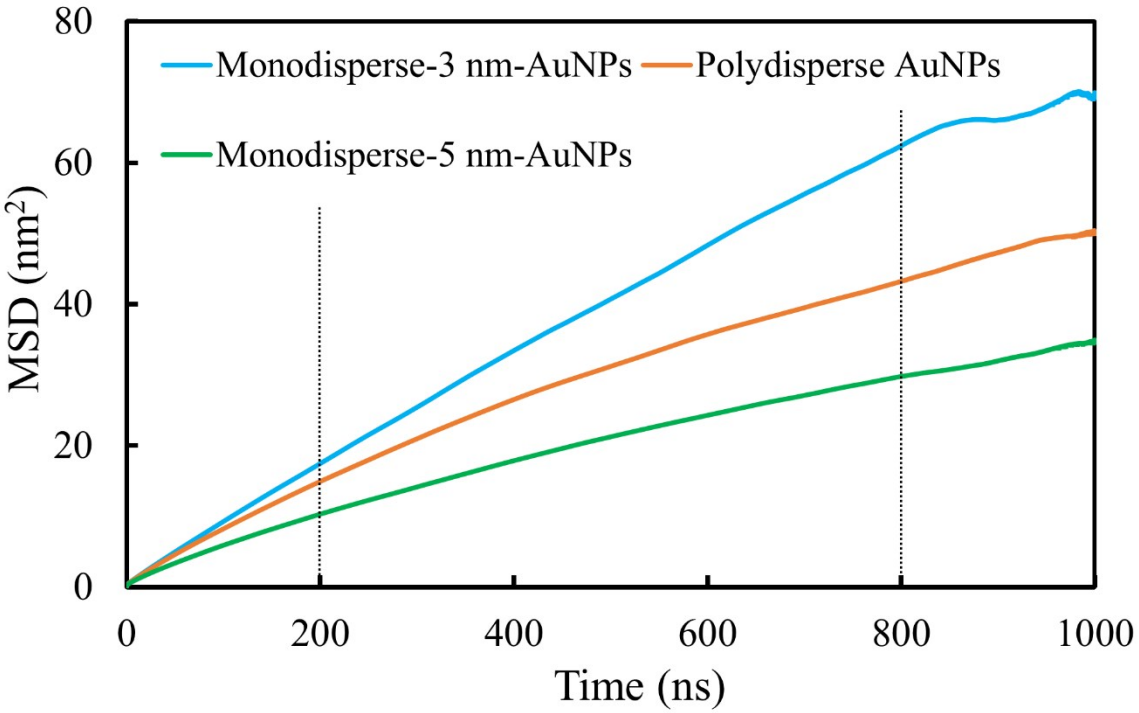

Fig. S15 MSD curves of phospholipids in the monolayer systems. These curves are for state II at ~0.58 mol%. The MSD for monodisperse 3 nm diameter AuNPs , monodisperse 5 nm diameter AuNPs and a polydisperse sample of 3 and 5 nm diameter AuNPs. The diffusion coefficients of the systems were obtained from the fitting of the MSD curves between the times denoted by the dotted lines.

Table S1. Effect of peptides (SP-B_{1-25}) on surface tension values of the surfactant monolayer in states I and II. All simulations performed with all AuNPs 3 nm in diameter.

Lung surfactant systems	AuNP concentration (mol %)	No. of AuNPs in each monolayer	Monolayer states	Constant	Variable	Pore formation
				APL / nm^2	Surface tension / mN/m^{-1}	
In the absence of peptide	~0.86	9	I	0.54	25.3±0.3	No
			II	0.47	25.2±0.7	No
In the presence peptide			I	0.54	27.5±0.4	No
			II	0.47	22.8±1.3	No

References:

1. B. Hess, *The Journal of Chemical Physics*, 2002, **116**, 209-217.
2. N. Nisoh, M. Karttunen, L. Monticelli and J. Wong-ekkabut, *RSC Advances*, 2015, **5**, 11676-11685.
3. H. J. C. Berendsen, J. P. M. Postma, W. F. v. Gunsteren, A. DiNola and J. R. Haak, *The Journal of Chemical Physics*, 1984, **81**, 3684-3690.
4. M. Parrinello and A. Rahman, *Journal of Applied physics*, 1981, **52**, 7182-7190.
5. http://manual.gromacs.org/documentation/5.1.4/manual-5.1.4.pdf (accessed June 2020).
6. Q. Hu, B. Jiao, X. Shi, R. P. Valle, Y. Y. Zuo and G. Hu, *Nanoscale*, 2015, **7**, 18025-18029.
7. L. S. Vermeer, B. L. de Groot, V. Réat, A. Milon and J. Czaplicki, *European Biophysics Journal*, 2007, **36**, 919-931.
8. L. Monticelli, S. K. Kandasamy, X. Periole, R. G. Larson, D. P. Tieleman and S.-J. Marrink, *J Chem Theory Comput*, 2008, **4**, 819-834.
9. S. I. Hossain, N. S. Gandhi, Z. E. Hughes and S. C. Saha, *MRS Advances*, 2019, **4**, 1177-1185.
10. S. I. Hossain, N. S. Gandhi, Z. E. Hughes, Y. T. Gu and S. C. Saha, *Biochimica et Biophysica Acta (BBA) - Biomembranes*, 2019, **1861**, 1458-1467.
11. E. D. Estrada-Lopez, E. Murce, M. P. P. Franca and A. S. Pimentel, *RSC Advances*, 2017, **7**, 5272-5281.

12. M. S. Bakshi, L. Zhao, R. Smith, F. Possmayer and N. O. Petersen, *Biophysical Journal*, 2008, **94**, 855-868.
13. E. D. Estrada-López, E. Murce, M. P. Franca and A. S. Pimentel, *RSC Advances*, 2017, **7**, 5272-5281.